

# Quantum Effect Induced Reverse Kinetic Molecular Sieving in Microporous Materials

A. V. Anil Kumar and Suresh K. Bhatia\*

*Division of Chemical Engineering, The University of Queensland, Brisbane, QLD 4072, Australia*

(Received 19 July 2005; published 9 December 2005)

We report kinetic molecular sieving of hydrogen and deuterium in zeolite rho at low temperatures, using atomistic molecular dynamics simulations incorporating quantum effects via the Feynman-Hibbs approach. We find that diffusivities of confined molecules decrease when quantum effects are considered, in contrast with bulk fluids which show an increase. Indeed, at low temperatures, a reverse kinetic sieving effect is demonstrated in which the heavier isotope, deuterium, diffuses faster than hydrogen. At 65 K, the flux selectivity is as high as 46, indicating a good potential for isotope separation.

DOI: [10.1103/PhysRevLett.95.245901](https://doi.org/10.1103/PhysRevLett.95.245901)

PACS numbers: 66.30.Pa, 68.43.Jk, 82.75.Jn

The molecular sieving properties of microporous materials such as zeolites, carbon molecular sieves, and other narrow pore materials have long been a subject of interest due to their technological importance and applications in separation [1]. Such molecular sieving is related to the size and shape of the guest molecules and of the subnanometer scale pores of the host solid, such that the permeability decreases dramatically for molecules larger than a critical size, thereby affecting kinetic separation. The most important such application is air separation, where the small difference in kinetic diameter between oxygen and nitrogen is sufficient to achieve kinetic separation using carbon molecular sieves or other suitable microporous materials, which has been industrially exploited. More recently, new nanoporous materials such as carbon nanotubes [2,3] also offer exciting possibilities in this direction, though relatively few studies with such materials exist [4–6].

Such narrow pore materials have, however, traditionally not been considered useful for isotope separation, a subject of considerable importance. Ostensibly, this is because, from a classical viewpoint, different isotopes have the same size and shape, and their diffusion properties differ only due to their different mass, suggesting infeasibility of size dependent separation. One such example is the separation of hydrogen isotopes, usually accomplished by more complex and energy consumptive distillation or thermal diffusion methods which rely on the difference in masses of the different isotopes. The traditional arguments, however, begin to fail when considering such light gases as  $H_2$  and  $D_2$ , because in these cases the degrees of freedom can no longer be treated classically when considering narrow pores comparable in size to the molecular diameter. In such a circumstance, the space available for molecular motion is highly restricted and comparable to the de Broglie wavelength, demanding a quantum treatment of the dynamics, particularly at low temperatures. Indeed, quantum considerations in equilibrium isotherm modeling have already demonstrated that heavier isotopes are more selectively adsorbed compared to lighter ones [7,8]. This equilibrium quantum sieving effect was first proposed by Beenakker *et al.* [9], using a simple square well potential model for

molecules in a cylindrical pore, predicting that radial degrees of freedom are frozen and the sorbate molecules act as a one-dimensional gas. Sholl and co-workers subsequently elaborated these effects in greater detail using more realistic models [7,10,11] in conjunction with theory and path integral-grand canonical Monte Carlo simulations, demonstrating very high selectivity for heavier isotopes compared to hydrogen in (10, 10) nanotubes and their interstitials. While this equilibrium behavior is to be expected, as quantum uncertainty will effectively lead to greater swelling of the lighter species ( $H_2$ ) and, thereby, to its relative exclusion, it is the extent of the selectivity enhancement that is the highlight of these studies. Here we show that the quantum effect on transport is far more spectacular and, under suitable conditions, leads also to kinetic molecular sieving favoring higher selectivity of the heavier species  $D_2$ , representing a dramatic reversal from the classical expectation that  $D_2$  diffuses slightly slower (by a factor of about  $\sqrt{2}$  in the Knudsen limit). This behavior, arising from a larger decrease in transport coefficient of  $H_2$ , due to a larger quantum effect, is also counter to that observed for bulk systems, where quantum effects have been shown to enhance self-diffusivity [12]. Indeed, this reverse kinetic molecular sieving effect is sufficiently significant for  $H_2/D_2$  mixtures as to offer an attractive option for their separation by molecular sieving. In particular, our results are based on simulations using a realistic system, that of zeolite rho, as opposed to the earlier equilibrium simulations with (3, 6) carbon nanotubes [7,8,10,11] that have yet to be synthesized.

All of the above earlier studies with confined systems have been directed at equilibrium properties, and, to the best of our knowledge, quantum effects on the dynamical properties of confined systems have not been investigated. Here we examine the latter, using equilibrium molecular dynamics (EMD) simulation with the Feynman-Hibbs (FH) modified interaction potential [13]

$$U_{FH}(r) = \left( \frac{6\mu}{\pi\beta\hbar^2} \right)^{3/2} \int d\mathbf{R} U(|\mathbf{r} + \mathbf{R}|) \exp\left( -\frac{6\mu}{\beta\hbar^2} R^2 \right) \quad (1)$$

that is based on a variational treatment of the path integral. Here  $U(r)$  is the classical pair potential, and Eq. (1) effectively considers the quantum pair as having a Gaussian spread of  $\sqrt{\beta\hbar^2/12\mu}$  in separation, where  $\mu$  is reduced mass and  $\beta = 1/k_B T$ . While path integral molecular dynamics provides a natural framework for investigating equilibrium as well as transport properties considering quantum effects, exploited in early studies of the equilibrium properties of bulk helium and neon [14,15], its excessive computational burden has prompted subsequent workers [12,16] to employ the above less demanding FH approach in their studies of quantum effects on transport of bulk fluids such as  $\text{H}_2\text{O}$ , He, Ne, and  $\text{CH}_4$ .

Our EMD simulations for hydrogen isotopes in zeolite rho model the sorbate and host atom-atom interactions by the Lennard-Jones (LJ) (12-6) potential. For the zeolite host whose cage and window structure is depicted in the inset in Fig. 1, the matrix is considered rigid, and the interaction of the oxygen atoms is considered dominant, following Yashonath and Santikary [17]. The unit cell structure was simulated based on the atom coordinates provided by Parise *et al.* [18]. For the  $\text{H}_2$ - $\text{H}_2$  and  $\text{D}_2$ - $\text{D}_2$  interaction, we use the parameters  $\sigma_f = 0.292$  nm and  $\varepsilon_f/k_B = 38$  K, while for the O- $\text{H}_2$  or O- $\text{D}_2$  interaction we use  $\sigma_{fO} = 0.273$  nm and  $\varepsilon_{fO}/k_B = 76.76$  K [19]. The simulations solve the system of first order differential equations  $\dot{\mathbf{q}}_i = \mathbf{P}_i/m$ ,  $\dot{\mathbf{P}}_i = \mathbf{F}_i - \lambda \mathbf{P}_i$ , where  $\lambda$  is the thermostat factor determined by the Gaussian principle of least constraint [20],  $\mathbf{q}_i$  and  $\mathbf{P}_i$  are the position and momentum vectors, respectively, and  $\mathbf{F}_i$  is the net force acting on the particle. The above equations are solved simultaneously using a fifth order Gear predictor corrector method with a 1 fs time step. The total run length of the simulations is typically 20 ns, in which the initial 500 ps is ignored in

calculating averages and dynamical properties, and each run typically comprises a system having about 768 fluid particles at a density of 1 particle per  $\alpha$  cage. The simulations have been carried out on an SGI Altix machine with an Itanium 1500 MHz CPU. A typical simulation run takes around 200 h of CPU time and 256 MB of memory, using FORTRAN-77 code. The transport diffusivity of the sorbate is determined from the autocorrelation of the streaming velocity, as discussed elsewhere [21].

In determining the effective potential considering quantum effects, Eq. (1) is replaced by

$$U_{\text{FH}}(r) = U(r) + \frac{\beta\hbar^2}{24\mu} \left( U''(r) + \frac{2U(r)}{r} \right) + \frac{\beta^2\hbar^4}{1152\mu^2} \left( \frac{15U'(r)}{r^3} + \frac{4U'''}{r} + U''''(r) \right), \quad (2)$$

obtained upon expanding the integrand in Eq. (1) in powers of  $R$  up to  $R^4$ . Equation (2) is used for the fluid-fluid as well as fluid-solid interactions. In addition to reducing computational time, the approximation overcomes the singularity in the integrand at zero interparticle separation. Such an approximation, but only considering a quadratic expansion, has been previously utilized for bulk systems [12,16] as well as in modeling gas-solid virial coefficients [22]. For the present case, where the adsorptive density is small (1  $\text{H}_2$ /cage), the fluid-fluid interaction is insignificant and the transport coefficient essentially corresponds to the zero density value. However, while the quadratic approximation has been found to produce results matching those from exact quantum calculations for the gas-solid interaction on a smooth structureless plane [22], our calculations showed the quadratic approximation to be inadequate, with Eq. (2) providing sufficient accuracy for the interaction in confined systems. As an example, for the exact Feynman-Hibbs modification of the one-dimensional cylindrical potential in a (3, 6) carbon nanotube using Eq. (1), the error associated with the quartic approximation is only about 2.3%, while that of quadratic approximation is 17.9%, at 65 K. This error increases with decreasing temperature and at 50 K reaches 8.9% and 53.7% for the quartic and quadratic approximations, respectively.

Our simulations of the transport in zeolite rho showed a striking contrast with bulk fluids, where quantum effects have been found to increase self-diffusivity of water [12] based on the FH potential. To the contrary, these effects lead to significant reduction in the diffusivity of the confined fluid, as illustrated in Fig. 1, depicting the temperature variation of the transport coefficient for both  $\text{H}_2$  and  $\text{D}_2$ , with the quantum diffusivity of  $\text{H}_2$  decreasing more strongly with temperature compared to the classical. Since fluid-fluid interactions are insignificant at low density, both self and transport diffusivities were identical, as expected. In the bulk fluid, the opposite effect, i.e., an increase of quantum diffusivity over classical, has been attributed to quantum tunneling, whereby a decrease of the intermolec-

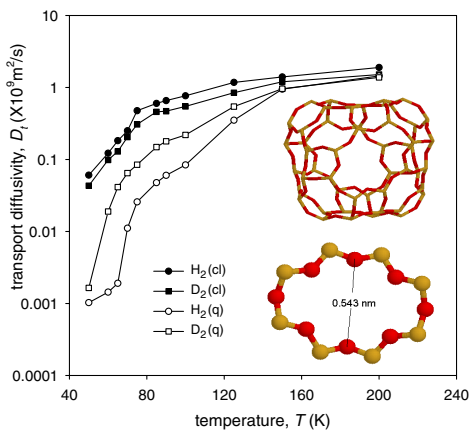


FIG. 1 (color online). Transport diffusivity of  $\text{H}_2$  (circle) and  $\text{D}_2$  (square) using classical (cl) LJ potential (solid symbols) and the quantum (q) FH potential (open symbols). The points are from the molecular dynamics simulations. The lines are guides to the eye. One  $\alpha$  cage of zeolite rho and an 8-ring window connecting two  $\alpha$  cages are shown as insets.

ular potential well depth reduces the translational energy barrier. Paradoxically, the confined quantum fluid suffers a reduction in the diffusivity despite a similar reduction in the well depth of the fluid-fluid and fluid-solid interactions. Figure 2 depicts the latter, which for the classical fluid is temperature independent and the same for both  $H_2$  and  $D_2$  but is temperature dependent for the quantum fluid, with  $H_2$  displaying the stronger effect consistent with its smaller mass. This decrease in the well depth is also associated with an increase in the effective size parameter of the fluid-fluid and fluid-solid quantum interactions, estimated as the separation at which the potential becomes zero and illustrated in the insets. In addition, the hardness of the fluid-solid interaction also concomitantly increases, as evidenced by the slope of the potential curve in the repulsive regime, whose magnitude increases from  $1623 \text{ K } \text{\AA}^{-1}$  in the classical case to  $2153 \text{ K } \text{\AA}^{-1}$  for the quantum fluid, for  $H_2$  at 50 K. All of these effects conspire to modify the diffusivity in different ways. In the first place, some increase in diffusivity is expected due to decrease in the well depth, following the theory of Bhatia and co-workers [23,24], since it makes the hydrogen or  $D_2$  more weakly adsorbing. The associated increase in hardness and of the value of the fluid-solid interaction size parameter also may be expected to contribute to an increase in the diffusivity by virtue of the related enhancement in specularity of reflections from the walls [5,25]. However, the dominant effect appears to be the steric hindrance caused by the increase in effective size parameter of the fluid-solid interaction, seen in the inset. Using the Berthelot rule, the classical fluid-solid size parameter has the value of  $0.273 \text{ nm}$ , so that  $H_2$  and  $D_2$  will be able to enter through windows as small as about  $0.5 \text{ nm}$ , assuming the minimum center to center separation is  $0.92\sigma_{sf}$  [24]. As shown in the inset in Fig. 1, the controlling size or bottleneck for the

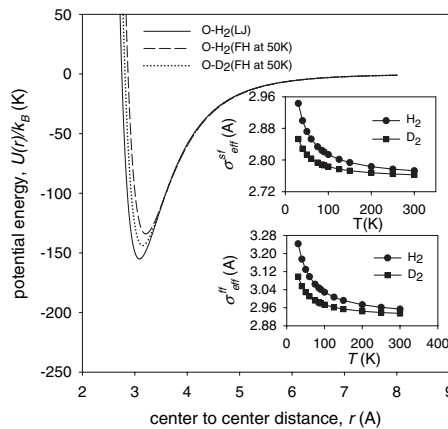


FIG. 2. The classical LJ potential (solid line) and the modified FH potential for  $H_2$  (dashed line) and  $D_2$  (dotted line) at 50 K. The temperature variations of the effective values of the size parameters for the solid-fluid ( $\sigma_{sf}$ ) and fluid-fluid ( $\sigma_{ff}$ ) interactions are shown as insets.

elliptical zeolite rho window is  $0.543 \text{ nm}$  (center to center separation of the oxygen atoms), so that the classical fluid will not be seriously hindered. On the other hand, as seen in the inset in Fig. 2, the quantum fluid-solid size parameter swells up to as much as  $0.282 \text{ nm}$  for hydrogen by 65 K and  $0.287 \text{ nm}$  at 50 K, with critical window sizes of  $0.519$  and  $0.528 \text{ nm}$ , respectively. Thus, with decrease in temperature as the controlling size of  $0.543 \text{ nm}$  is approached, the diffusivity can be expected to reduce drastically for hydrogen. On the other hand, for the heavier  $D_2$ , the quantum effects are weaker, and the critical window size increases from  $0.511$  to  $0.518 \text{ nm}$  over this temperature range, explaining the higher diffusivity of  $D_2$  at these temperatures. Of all the above effects, for the bulk fluid only the well-depth decrease effect applies, leading to the quantum-tunneling related diffusivity enhancement.

Among the remarkable features of the above results is the extent of the drop in transport coefficient of hydrogen relative to deuterium which, as seen in Fig. 1, leads to the heavier  $D_2$  diffusing faster below  $150 \text{ K}$ , representing a reverse kinetic molecular sieving. This is easily reconciled by the potential energy curves in Fig. 2, which show that the quantum shift in the potential is smaller for  $D_2$  compared to  $H_2$ , and, therefore, the swelling of  $D_2$  is smaller, by virtue of its larger mass. This leads to increase in kinetic selectivity for  $D_2$  (defined as  $[D_2]_{D_2}/[D_2]_{H_2}$ ) with reduction in temperature. Figure 3 depicts this selectivity variation with temperature, showing a dramatic increase in the quantum selectivity below about  $70 \text{ K}$ , with a peak value of  $21.70$  at about  $65 \text{ K}$ , below which it decreases. The latter decrease is due to the stronger decrease of the transport coefficient for  $D_2$ , for which the quantum effects begin to assume significance, as seen by the more rapid increase in the associated value of  $\sigma_{sf}$  in the inset in Fig. 2.

Concomitant with the above low-temperature kinetic selectivity enhancement for  $D_2$ , one anticipates the relative increase in size of  $H_2$ , and decrease in its well depth, to lead to an increase in the equilibrium selec-

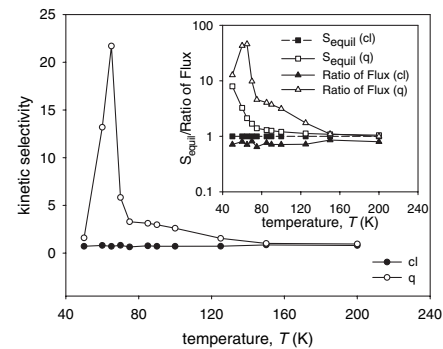


FIG. 3. Classical and quantum kinetic selectivity of  $D_2$  to  $H_2$  in zeolite rho against temperature. The classical (cl) and quantum (q) equilibrium selectivity (squares) and ratio of flux (triangle) are given as an inset. Again, the classical values are denoted by solid symbols and quantum values by open symbols.

tivity of  $D_2$ , defined by  $S_e = [\int \exp(-\beta\phi_{fs}(r)d\mathbf{r})_{D_2} / \int \exp(-\beta\phi_{fs}(r)d\mathbf{r})_{H_2}]$ , as is observed for carbon nanotubes and their interstitial space [7,8]. The inset in Fig. 3 confirms this behavior, with the quantum selectivity increasing tenfold at 50 K, while the classical selectivity is constant at unity. Although this result suggests some potential for low-temperature adsorption based separation of  $D_2$  and  $H_2$  using zeolite rho, a somewhat more attractive proposition would appear to be a supported zeolite rho membrane based separation, for which the indicative selectivity, given as the ratio of fluxes, may be defined as the ratio of the products of equilibrium and kinetic selectivity. The inset in Fig. 3 depicts the variation of this  $D_2:H_2$  flux selectivity with temperature which, while entirely unattractive from a classical perspective, is highly significant and as high as 46 at 65 K, for the quantum fluid. In comparison with the hypothetical (3,6) nanotubes hitherto examined from an equilibrium context, the present proposal appears more attractive and feasible.

In our simulations, we have considered the solid matrix as rigid. Investigations on the transport of adsorbates in different zeolite systems remain inconclusive about the effect of lattice vibrations [26–28]. While Demontis and co-workers report very small influence of lattice vibrations on the diffusivity at low density [27,28], Jakobtorweihen *et al.* find a rather significant effect of lattice vibrations on diffusion in carbon nanotubes at low density [29], with the diffusivity in flexible carbon nanotubes being significantly smaller than that for rigid nanotubes. In the present case, lattice vibrations will have a stronger effect on  $H_2$  than on  $D_2$  because of the larger effective collision cross section of the former at low temperatures. Consequently, the diffusivity of  $H_2$  will decrease more than that of  $D_2$ , thereby enhancing the kinetic selectivity obtained here.

In conclusion, atomistic molecular dynamics simulations incorporating quantum effects following the Feynman-Hibbs variational approach demonstrate quantum mediated reverse kinetic molecular sieving for  $H_2/D_2$  mixtures in nanoporous materials of sufficiently small pore dimension at low temperatures. These results hold promise for new separation processes exploiting this quantum effect.

---

\*To whom all correspondence should be addressed.

Electronic address: sureshb@cheque.uq.edu.au

- [1] J. Karger and D.M. Ruthven, *Diffusion in Zeolites and Other Microporous Materials* (Wiley, New York, 1992).
- [2] S. Iijima, *Nature* (London) **354**, 56 (1991).

- [3] R. Saito, G. Dresselhaus, and M. S. Dresselhaus, *Physical Properties of Carbon Nanotubes* (Imperial College Press, London, 1998).
- [4] A. I. Skoulidas, D. M. Ackerman, J. K. Johnson, and D. S. Sholl, *Phys. Rev. Lett.* **89**, 185901 (2002).
- [5] S. K. Bhatia, H. B. Chen, and D. S. Sholl, *Mol. Simul.* **31**, 643 (2005).
- [6] B. J. Hinds, N. Chopra, T. Rantell, R. Andrews, V. Gavalas, and L. G. Bachas, *Science* **303**, 62 (2004).
- [7] Q. Y. Wang, S. R. Challa, D. S. Sholl, and J. K. Johnson, *Phys. Rev. Lett.* **82**, 956 (1999).
- [8] H. Tanaka, H. Kanoh, M. El-Merraoui, W. A. Steele, M. Yudasaka, S. Iijima, and K. Kaneko, *J. Phys. Chem. B* **108**, 17457 (2004).
- [9] J. J. M. Beenakker, V. D. Borman, and S. Y. Krylov, *Chem. Phys. Lett.* **232**, 379 (1995).
- [10] S. R. Challa, D. S. Sholl, and J. K. Johnson, *Phys. Rev. B* **63**, 245419 (2001).
- [11] S. R. Challa, D. S. Sholl, and J. K. Johnson, *J. Chem. Phys.* **116**, 814 (2002).
- [12] B. Guillot and Y. Guissani, *J. Chem. Phys.* **108**, 10162 (1998).
- [13] R. P. Feynman and A. R. Hibbs, *Quantum Mechanics and Path Integrals* (McGraw-Hill, New York, 1965).
- [14] K. Singer and W. Smith, *Mol. Phys.* **64**, 1215 (1988).
- [15] E. L. Pollock and D. M. Ceperley, *Phys. Rev. B* **30**, 2555 (1984).
- [16] N. Tchouar, F. Ould-Kaddour, and D. Levesque, *J. Chem. Phys.* **121**, 7326 (2004).
- [17] S. Yashonath and P. Santikary, *J. Phys. Chem.* **98**, 6368 (1994).
- [18] J. B. Parise, L. Abrams, T. E. Gier, D. R. Corbin, J. D. Jorgensen, and E. Price, *J. Phys. Chem.* **88**, 2303 (1984).
- [19] A. V. Kiselev and P. Q. Du, *J. Chem. Soc., Faraday Trans. 2* **77**, 1 (1981).
- [20] D. J. Evans and G. P. Morriss, *Statistical Mechanics of Nonequilibrium Liquids* (Academic, London, 1990).
- [21] S. K. Bhatia and D. Nicholson, *Phys. Rev. Lett.* **90**, 016105 (2003).
- [22] X-P. Jiang and M. Cole, *Phys. Rev. B* **33**, 2803 (1986).
- [23] O. G. Jepps, S. K. Bhatia, and D. Bernhardt, *Phys. Rev. Lett.* **91**, 126102 (2003).
- [24] S. K. Bhatia, O. G. Jepps, and D. Nicholson, *J. Chem. Phys.* **120**, 4472 (2004).
- [25] G. Arya, H. C. Chang, and E. D. Maginn, *Mol. Simul.* **29**, 697 (2003).
- [26] D. I. Kopelevich and H.-C. Chang, *J. Chem. Phys.* **114**, 3776 (2001).
- [27] P. Demontis, G. B. Suffritti, E. S. Foiss, and S. Quartieri, *J. Phys. Chem.* **96**, 1482 (1992).
- [28] S. Fritzsche, M. Wolfsberg, R. Haberlandt, P. Demontis, G. B. Suffritti, and A. Tilocca, *Chem. Phys. Lett.* **296**, 253 (1998).
- [29] S. Jakobtorweihen, M. G. Verbeek, C. P. Lowe, F. J. Keil, and B. Smit, *Phys. Rev. Lett.* **95**, 044501 (2005).